JGR Atmospheres

RESEARCH ARTICLE
10.1029/2021JD034671

Methane Emissions Offset Net Carbon Dioxide Uptake From an Alpine Peatland on the Eastern Qinghai-Tibetan Plateau

Haijun Peng[1,2,3,4], Jinshu Chi[2], Hu Yao[1,4,5], Qian Guo[1,4,5], Bing Hong[1,4,5], Hanwei Ding[1,4,5], Yongxuan Zhu[1], Jie Wang[1,4,5], and Yetang Hong[1]

[1]State Key Laboratory of Environmental Geochemistry, Institute of Geochemistry, Chinese Academy of Sciences, Guiyang, China, [2]Department of Forest Ecology and Management, Swedish University of Agricultural Sciences, Umeå, Sweden, [3]Bayinbuluk Alpine Wetland Carbon Flux Research Station, Chinese Flux Observation and Research Network, Beijing, China, [4]CAS Center for Excellence in Quaternary Science and Global Change, Xi'an, China, [5]University of Chinese Academy of Sciences, Beijing, China

Key Points:

- CH_4 emissions offset the net CO_2 uptake from an alpine peatland on eastern Qinghai-Tibetan Plateau
- The alpine peatland showed a net radiative warming effect
- Global radiation and soil temperature were dominant abiotic controls of net CO_2-eq flux variations

Supporting Information:

Supporting Information may be found in the online version of this article.

Correspondence to:

J. Chi and B. Hong,
jinshu.chi@slu.se;
hongbing@mail.gyig.ac.cn

Citation:

Peng, H., Chi, J., Yao, H., Guo, Q., Hong, B., Ding, H., et al. (2021). Methane emissions offset net carbon dioxide uptake from an alpine peatland on the eastern Qinghai-Tibetan Plateau. *Journal of Geophysical Research: Atmospheres*, *126*, e2021JD034671. https://doi.org/10.1029/2021JD034671

Received 27 JAN 2021
Accepted 18 SEP 2021

Abstract Peatlands store large amounts of carbon (C) and actively exchange greenhouse gases (GHGs) with the atmosphere, thus significantly affecting global C cycle and climate. Large uncertainty exists in C and GHG estimates of the alpine peatlands on Qinghai-Tibetan Plateau (QTP), as direct measurements of CO_2 and CH_4 fluxes are scarce in this region. In this study, we provided 32-month CO_2 and CH_4 fluxes measured using the eddy covariance (EC) technique in a typical alpine peatland on the eastern QTP to estimate the net C and CO_2 equivalent (CO_2-eq) fluxes and investigate their environmental controls. Our results showed that the mean annual CO_2 and CH_4 fluxes were −68 ± 8 g CO_2-C m^{-2} yr^{-1} and 35 ± 0.3 g CH_4-C m^{-2} yr^{-1}, respectively. While considering the traditional and sustained global warming potentials of CH_4 over the 100-year timescale, the peatland acted as a net CO_2-eq source (1,059 ± 30 and 1,853 ± 31 g CO_2-eq m^{-2} yr^{-1}, respectively). The net CO_2-eq emissions during the non-growing seasons contributed to over 40% of the annual CO_2-eq budgets. We further found that net CO_2-eq flux was primarily influenced by global radiation and soil temperature variations. This study was the first assessment to quantify the net CO_2-eq flux of the alpine peatland in the QTP region using EC measurements. Our study highlights that CH_4 emissions from the alpine peatlands can largely offset the net cooling effect of CO_2 uptake and future climate changes such as global warming might further enhance their potential warming effect.

1. Introduction

Carbon dioxide (CO_2) and methane (CH_4) are the two most important long-lived greenhouse gases (LLGHGs) and together contribute to over 80% of the radiative forcing caused by LLGHGs (WMO, 2018). Peatlands cover only about 3% of the Earth's land surface area but store over 614 ± 80 Pg (10^{15} g) of carbon (C), accounting for one-third of the global soil C pool and about 70% of the atmospheric C pool (Loisel et al., 2017; Xu et al., 2018; Yu, 2011; Yu et al., 2010). It has been widely acknowledged that peatlands have played an important role in regulating the global C and GHG cycles and climate change (Friedlingstein et al., 2019; Frolking et al., 2011; Hopple et al., 2020). Peatland ecosystems have the potential to mitigate climate change by sequestering CO_2 from the atmosphere into biomass and soils (Baldocchi & Penuelas, 2019; Nugent et al., 2019; Stocker et al., 2017); meanwhile, peatlands emit large amounts of CH_4 to the atmosphere during the peatland forming and growing processes (Dommain et al., 2018; Kirschke et al., 2013), thus resulting in contrasting effects on radiative forcing. Both pathways are sensitive to climate change and anthropogenic activities (Chen et al., 2013; Frolking et al., 2011); for example, drought caused by both peatland drainage and low precipitation (Fenner & Freeman, 2011; Swindles et al., 2019), peatland wildfires and burning (Turetsky et al., 2015), and conversion for agricultural uses (Carlson et al., 2013; Dommain et al., 2018) can shift the peatlands from net GHG sinks to sources. However, it should be noted that the historical, current, and future contributions of peatlands to the global C budget and radiative forcing are still uncertain due to limited knowledge of the synergistic feedbacks of CO_2 and CH_4 to climatic perturbation and anthropogenic activities (Luan et al., 2018; Petrescu et al., 2015; Stocker et al., 2017).

The uncertainty in CO_2 and CH_4 stoichiometry of peatlands could be attributed to a variety of sources, such as the lack of reliable global peatland area estimates (Chaudhary et al., 2017; Xu et al., 2018; Yu et al., 2010), difficulties in quantifying terrestrial anaerobic or oxidative sources and sinks (Bridgham et al., 2013; Loisel et al., 2017; Poulter et al., 2017), and the scarcity of both CO_2 and CH_4 flux measurements, especially from low-latitude and high-altitude peatlands (Bridgham et al., 2013; Kirschke et al., 2013; Schaefer et al., 2016; Yu et al., 2010). To date, most of the peatland C fluxes have been measured in the northern high-latitude (45–70°N; Loisel et al., 2017; Turetsky et al., 2014). Recent studies show that wetland ecosystems in the subtropical and tropical regions have acted as C sinks, but their CH_4 emissions can offset net CO_2 uptake under warm scenarios, thus contributing to a positive radiative forcing (Dalmagro et al., 2019; Dommain et al., 2018; J. Liu et al., 2020). Considering peatlands in the low-latitude regions have a sizable amount of C stocks and higher CH_4 emissions and CO_2 uptake rates compared to the northern peatlands (Loisel et al., 2017; Nilsson et al., 2008; Yu et al., 2010), the lack of C flux measurements from these areas could lead to large uncertainty in the global peatland C and GHG budget estimations (X. Liu et al., 2019; Schaefer et al., 2016; Turetsky et al., 2015). Therefore, more monitoring is needed to reveal the dynamics in peatland-atmosphere C exchanges and dynamics.

The Ruoergai peatland in the eastern margin of the Qinghai-Tibetan Plateau (QTP) is the largest consecutive alpine peatland in the world, covering a total area of 4,600 km^2 at an average elevation of 3,400 m above sea level (Chen et al., 2014; Xiang et al., 2009; L. Yao et al., 2011). The climate of the eastern QTP is influenced by the Asian monsoons and characterized by short, warm, and wet summer with high solar irradiation and long, cold, and dry winter, which promotes the growth of herbaceous plants and preserving of peat or organic material rich soils (Hong et al., 2005; Peng et al., 2015). The mean annual temperature in the QTP region has been rapidly increasing at a rate of 0.27°C per decade during 1961–2005, which is four times higher than the increasing rate of global mean temperature (Tang et al., 2018; You et al., 2016). Due to the rapid warming, glacier melting and retreats have provided more water for peatland formation despite precipitation in the QTP region has not changed dramatically (T. Yao et al., 2012). As the biogeochemical processes regulating the CO_2 and CH_4 flux magnitudes are temperature-dependent and sensitive to water availability (Hopple et al., 2020; Peichl et al., 2014; Yuan et al., 2011; Yvon-Durocher et al., 2014), both fluxes can be significantly altered due to climate change in the QTP region (Chen et al., 2013; Yang et al., 2014).

The C balance and radiative forcing of peatlands from decadal to millennial timescales have been well understood in some regions of the globe (Frolking & Roulet, 2007; Johansson et al., 2006; Mathijssen et al., 2017; Minkkinen et al., 2002). Yet, studies into seasonal, annual, and between-years variabilities of wetland net CO_2 equivalent flux (net CO_2-eq flux, i.e., summing up CO_2 and CH_4 fluxes weighted by different global warming potential [GWP] metrics of CH_4) and its overall environmental controls are still rare (Dalmagro et al., 2019; Dommain et al., 2018; J. Liu et al., 2020), even entirely lacking in the QTP alpine peatlands. In this study, we compiled 32 months of continuous eddy covariance (EC) measurements of CO_2 and CH_4 fluxes at a typical alpine peatland on the eastern QTP to (a) characterize the temporal variations of net ecosystem exchanges of CO_2, CH_4, and their CO_2 equivalents between the alpine peatland and the atmosphere; (b) investigate the biophysical drivers of the net CO_2-eq fluxes at different temporal scales; and (c) assess the overall net radiative forcing arising from sustained CH_4 emissions and concurrent net CO_2 uptake from the alpine peatland on the eastern QTP. To our knowledge, this study was the first to present a multi-year continuous data set of ecosystem-scale net CO_2-eq flux over alpine peatlands on QTP, providing key information for understanding the role of alpine peatlands in the global C balance and net radiative forcing.

2. Methods

2.1. Site Description

The study site is located at the Hongyuan Peatland Carbon Flux Monitoring and Research Station (32°46′ N, 102°30′E, 3,510 m.a.s.l.) and operated by the Institute of Geochemistry, Chinese Academy of Sciences. The site is located in a valley on the eastern side of the Bai River in Hongyuan County, Sichuan Province, China (Figure 1). The Hongyuan peatland extends across an area of 1.1 km^2 and the deepest peat deposition is around 6.5 m. It is a part of the Ruoergai wetland, which covers 15% of the Ruoergai Basin area on the eastern QTP (Peng et al., 2019; L. Yao et al., 2011) and stores approximately 0.48 Pg C, some of which have

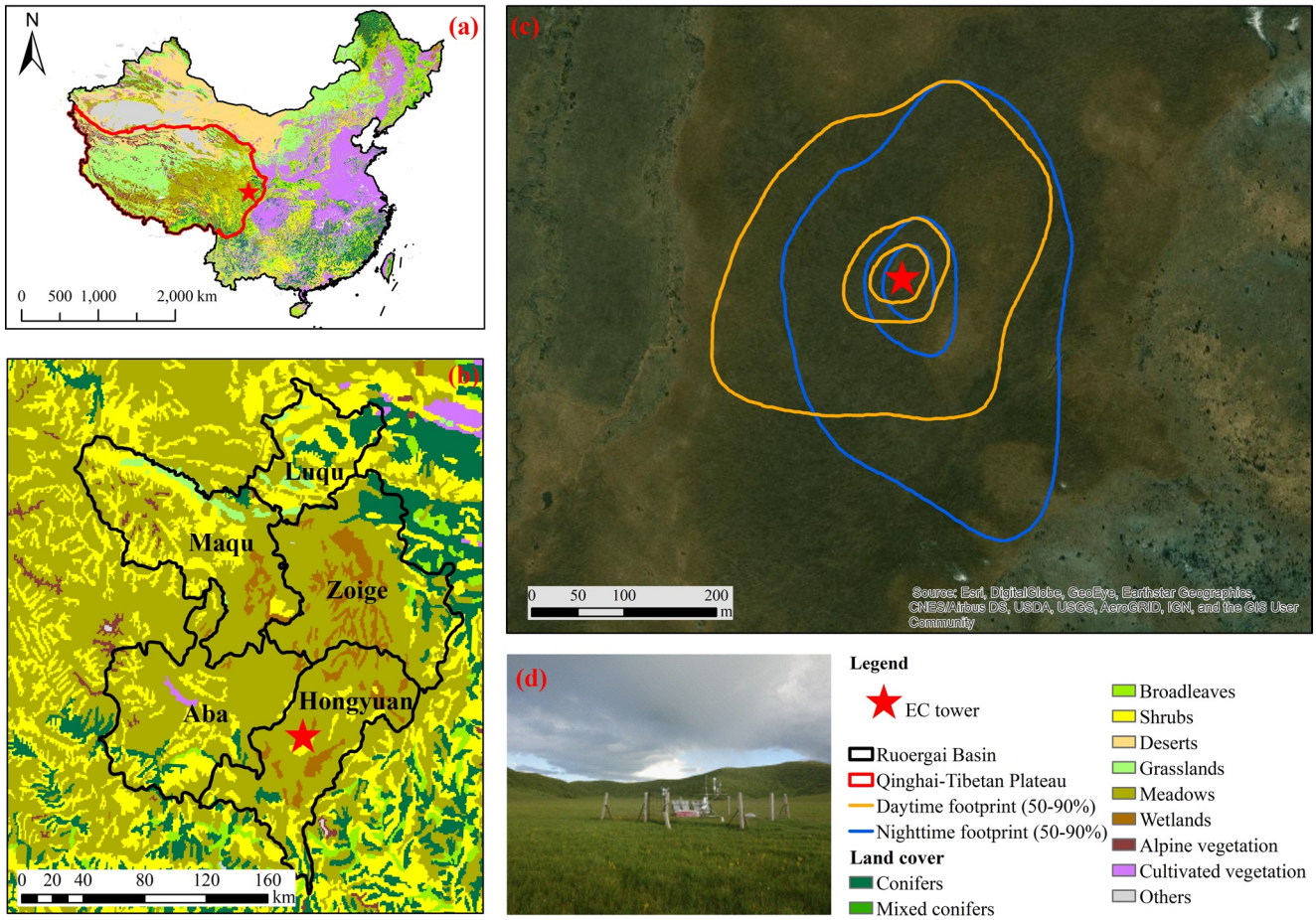

Figure 1. Location of the eddy covariance flux tower at Hongyuan peatland on the eastern Qinghai-Tibetan Plateau and its flux measurement footprint during daytime (orange lines) and nighttime (blue lines). The land cover data in panels (a and b) were retrieved from the Data Center for Resources and Environmental Sciences of the Chinese Academy of Sciences (http://www.csdb.cn). The footprint contour lines in panel (c) are shown in increments of 20% from 50% (inner circle) to 90% (outer circle). The typical landscape of Hongyuan peatland and a view of the EC station in the growing season were illustrated in panel (d).

been formed since 15,000 years ago (Chen et al., 2014). The long-term (1981–2010) meteorological data from the National Benchmark Climate Station in Hongyuan (http://data.cma.cn/) showed the regional climate pattern that the mean annual temperature and precipitation are 1.8°C and 746 mm, respectively. The highest monthly mean air temperature is typically observed in July (11.2°C on average) in this region, whereas the lowest is in January with a 30-year mean of −9.4°C. Over 75% of the annual precipitation usually occurs during the growing season from May to September each year. The dominant plant species in Hongyuan peatland are *Carex mulieensis* and *Kobresia tibetica*, and other abundant plant species include *Caltha palustris*, *Gentiana formosa*, and *Trollius farreri*.

2.2. Eddy Covariance and Ancillary Measurements

The EC and ancillary data were continuously measured from December 2013 to July 2016. The EC tower was installed in the center of Hongyuan peatland, where the terrain is flat and the average peat depth is 3.3 m. The flat area has a diameter of >300 m, which provides a homogeneous upwind fetch for the EC flux measurements (Figure 1c). The EC sensors were mounted at 2.5 m above the ground, consisting of a 3-D ultrasonic anemometer (WindMaster Pro, Gill Instruments Limited) for measuring wind components, an open-path infrared gas analyzer (LI-7500A, LI-COR Biosciences) for measuring carbon dioxide and water vapor densities, and an open-path gas analyzer (LI-7700, LI-COR Biosciences) for measuring CH_4 concentrations. The LI-7500A was tilted 10° in the main wind direction to avoid water accumulation on the lens. The raw EC data were recorded at 10 Hz using the LI-7550 data logger (LI-COR Biosciences). Other

ancillary environmental measurements, including global radiation (R_g), air temperature (T_{air}) and relative humidity (RH), precipitation (PPT), soil temperature (T_{soil}) at three depths (10, 25, and 40 cm below the ground), and soil water content (SWC) at a depth of 10 cm, were recorded by a HOBO U30 weather station installed near the EC tower (Figure 1d). Vapor pressure deficit (VPD) was calculated using the T_{air} and RH measurements. The EC tower was powered by solar panels during daytime and lead-acid batteries during nighttime or when solar radiation was low. A more detailed description of instrumentation is presented in Peng et al. (2019).

2.3. Flux Data Processing and Radiative Forcing Calculation

The 10 Hz EC raw data were processed using the EddyPro® software (Version 7.0.6, LI-COR Biosciences) to obtain the half-hourly averaged fluxes of CO_2 and CH_4. In brief, double rotation (Wilczak et al., 2001), block average (Gash & Culf, 1996), and covariance maximization (Fan et al., 1990) were applied in the EddyPro settings. Flux data were corrected for spectral attenuations (Moncrieff et al., 1997, 2004) and density fluctuations (Webb et al., 1980). The self-heating correction (Burba et al., 2008) for the LI-7500A open-path analyzer was not applied at this site, as it had negligible effects on our CO_2 and CH_4 fluxes (Figure S1). The 30-min CO_2 and CH_4 flux data were filtered according to the "0-1-2" quality check flagging policy (Mauder & Foken, 2004) that data with a flag of "2" were discarded. As spikes still occurred in the time series data, half-hourly CO_2 and CH_4 fluxes were further filtered if they were outside the range of mean $\pm$ 3 $\times$ standard deviation over a moving window of 10 days. Moreover, the half-hourly CO_2 flux data measured during the calm and stable atmospheric conditions, indicated by low friction velocity (u_*) were discarded via the REddyProc online tool (Wutzler et al., 2018) following the procedures described in Papale et al. (2006). The average u_* threshold was 0.084 m s^{-1} with a range of 0.079–0.099 m s^{-1} at our site. The effects of u_* threshold selection on cumulative gap-filled CO_2 flux data were shown in Figure S2. The same u_* thresholds estimated for CO_2 flux were also applied to filter CH_4 flux data. During the measurement period, 21% of CO_2 and CH_4 flux data were lost due to sensor malfunctioning, 14% of CO_2 and 11% of CH_4 flux data were filtered due to the steady state and developed turbulent condition tests (Mauder & Foken, 2004), 7% of CO_2 and 8% of CH_4 flux data were discarded due to this u_*-filtering approach, and another 2% of CO_2 and 9% of CH_4 flux data were filtered due to the statistical outliers. Overall, 56% of CO_2 and 51% of CH_4 flux data were retained as good quality data. The monthly gap fractions were shown in a greater detail in Figure S3.

Gaps in CO_2 flux were filled using the marginal distribution sampling (MDS) method (Reichstein et al., 2005) implemented in the REddyProc online tool. The MDS look-up table variables include global radiation, air temperature, and VPD. As CH_4 emissions are widely found to be controlled by soil temperature and water table level (e.g., Chen et al., 2021; Rinne et al., 2018; Ueyama et al., 2020), the CH_4 flux data were gap-filled by the regression fitting approach using soil temperature and SWC as environmental drivers. More details are provided in our previous study (Peng et al., 2019). The micrometeorological sign convention was used in this study that positive and negative fluxes indicated emission from and uptake by the peatland ecosystem, respectively.

The net radiative forcing of Hongyuan peatland was computed as the sum of the vertical CO_2 and CH_4 fluxes in CO_2 equivalents (defined as net CO_2-eq flux) weighted by GWP of CH_4. We applied both the traditional and sustained GWP (SGWP) metrics, the latter of which has been recently used to determine the net radiative forcing of several ecosystems by considering their persistent GHG emissions rather than the isolated pulse emissions (e.g., Hemes et al., 2018, 2019; J. Liu et al., 2020). In this study, we chose the CH_4 GWP of 28 CO_2-eq (GWP-28) without the inclusion of climate-carbon feedbacks (Myhre et al., 2013) and the SGWP of 45 CO_2-eq (SGWP-45) (Neubauer & Megonigal, 2015) over the 100-year time horizon. A positive net CO_2-eq value indicates an overall climatic warming effect and vice versa.

2.4. Flux Uncertainty, Statistical, and Footprint Analyses

Flux uncertainties due to the random measurement errors and gap-filling methods were estimated for CO_2 and CH_4 fluxes, respectively. The random measurement errors (σ_{rm}) in half-hourly CO_2 and CH_4 fluxes were obtained from the EddyPro output using the approach described in Finkelstein and Sims (2001). The half-hourly CO_2 and CH_4 flux uncertainties due to gap-filling (σ_{gf}) were estimated separately due to the

different gap-filling methods. We applied the Monte Carlo simulation (100 repetitions) approach following the procedures from Richardson and Hollinger (2007) to estimate the σ_{gf} in CO_2 flux by calculating the standard deviations of the 100 half-hourly CO_2 flux data sets. The half-hourly σ_{gf} in CH_4 flux was estimated using the bias errors (i.e., the difference between the modeled and measured CH_4 fluxes). The half-hourly total flux uncertainty was calculated by error propagation of σ_{rm} and σ_{gf}. The half-hourly errors were further summed by squares to obtain the daily, monthly, and yearly cumulative errors.

Principle component analysis (PCA) was performed on the time-series data at the temporal resolutions of 30-min (non-gapfilled), daily, and monthly to investigate the correlation structures of the CO_2, CH_4, and net CO_2-eq fluxes with the environmental variables. Flux measurement footprint was estimated using the two-dimensional footprint parametrization (Kljun et al., 2015). Roughness length (z_0) and zero-plane displacement height (d) were estimated as 1/10 and 2/3 of the canopy height (0.1 m), respectively. Besides, other footprint model input includes wind direction, standard deviation of lateral wind component fluctuations, friction velocity, Monin-Obukhov length, and atmospheric boundary layer height, that is, 800 and 200 m for daytime-condition and nighttime-condition, respectively, for the eastern QTP region (Slättberg & Chen, 2020).

2.5. Evaluation Periods

During the study period from December 2013 to July 2016, the annual period is defined as the calendar year, which is further divided into four seasons based on the approaches described in Aurela et al. (2002) and Lund et al. (2010). The first and last dates of growing season (GS) were the first day with daily mean $T_{air} > 5$ and <5°C for 7 consecutive days, respectively. The start and end of winter (W) were defined as the first day with daily mean T_{soil} at the depth of 10 cm was below and above 0°C for 2 consecutive days, respectively. Soil thawing (ST) incorporated the time period between winter and growing season and soil freezing (SF) extended from the end of the growing season to the beginning of the winter. The starting and ending dates and length for each season during the study period were listed in the Supporting Information (Table S1).

3. Results

3.1. Environmental Conditions

The environmental conditions showed distinct characteristics between the two full annual periods (Figure 2). As shown in Figure 2a, T_{air} did not differ much between the 2 years ($p > 0.05$), but the mean R_g during 2015 was significantly higher than in 2014 ($p < 0.05$), especially during the growing season. Compared to 2014, the year of 2015 was identified as a dry year, with 182 mm less PPT occurring during the growing season. However, the cumulative PPT during the first half of the growing season (May–July) was similar in 2014 and 2015 (316 vs. 334 mm), and thus the largely reduced PPT mainly occurred from August 2015 (Figure 2b). During the first half of the growing season, T_{soil} at the depth of 10 cm decreased by 1.0°C from 2014 to 2015, forming a cooler and wetter soil condition over that period due to a slight increase in PPT. In contrast to the growing season, T_{soil} at 10 cm deep was on average 0.53°C warmer during the non-growing season in 2015 (1.21°C) compared to 2014 (0.68°C). As expected, SWC mainly varied with PPT throughout the study period (Figure 2c).

3.2. Temporal Patterns of CO_2 and CH_4 Fluxes

The peatland was a net CO_2 sink from May or June to September each year but a net source of CH_4 throughout the entire study period (Figure 3). Combining both CO_2 and CH_4 fluxes into CO_2 equivalents using the GWP-28 metric, the peatland acted as a net source of CO_2-eq fluxes for 10 and 11 months during 2014 and 2015, respectively. The lowest net CO_2-eq flux concurred with the highest CO_2 uptake in July each year, around which the highest monthly CH_4 fluxes were also observed, that is, in August 2014, July 2015, and July 2016. The peak net CO_2-eq emission was observed at the end of the growing season each year, that is, September 2014 and October 2015. While applying the SGWP-45 metric, the monthly net CO_2-eq fluxes

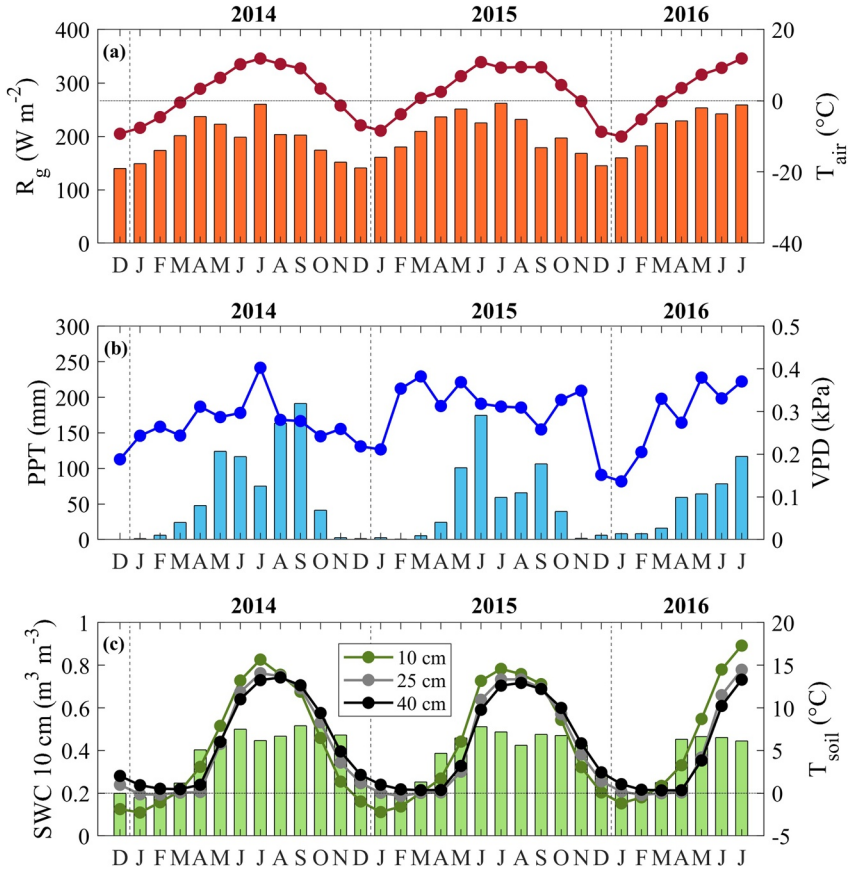

Figure 2. Monthly means (or sums) of environmental variables during the study period from December 2013 to July 2016 at Hongyuan peatland. (a) Monthly mean global radiation (R_g, red bars) and air temperature (T_{air}, red dots); (b) monthly precipitation sums (PPT, cyan bars) and monthly mean vapor pressure deficit (VPD, blue dots); and (c) monthly mean soil water content at a depth of 10 cm (SWC, green bars) and soil temperature (T_{soil}) at the depths of 10 cm (green dots), 25 cm (gray dots), and 40 cm (black dots).

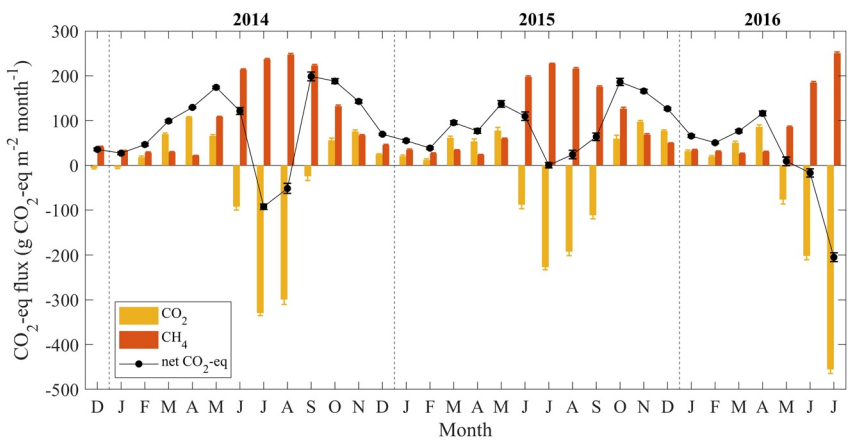

Figure 3. Monthly sums of CO_2, CH_4, and net CO_2-eq (GWP-28) fluxes over the study period from December 2013 to July 2016 at Hongyuan peatland. All flux components are in g CO_2-eq m^{-2} month^{-1} using CH_4 traditional global warming potential of 28 (GWP-28). The error bars represent the flux uncertainties due to random measurement errors and gap-filling methods.

Table 1
Seasonal and Annual Statistics of CO_2 and CH_4 Fluxes, and Their CO_2 Equivalents at Hongyuan Peatland

		CO_2 flux		CH_4 flux			Net C or CO_2-eq flux		
	Year	g C m^{-2} (d^{-1})	g CO_2 m^{-2} (d^{-1})	g C m^{-2} (d^{-1})	g CO_2-eq m^{-2} (d^{-1}) (GWP-28)	g CO_2-eq m^{-2} (d^{-1}) (SGWP-45)	g C m^{-2} (d^{-1})	g CO_2-eq m^{-2} (d^{-1}) (GWP-28)	g CO_2-eq m^{-2} (d^{-1}) (SGWP-45)
A_{sum}	2014	−91 *(5)*	−334 *(19)*	37 *(0.2)*	1,381 *(6)*	2,220 *(10)*	−54 *(5)*	1,047 *(20)*	1,886 *(21)*
	2015	−44 *(6)*	−161 *(21)*	33 *(0.2)*	1,232 *(6)*	1,980 *(10)*	−11 *(6)*	1,071 *(22)*	1,819 *(23)*
A_{mean}	2014	−0.25 *(0.01)*	−0.92 *(0.05)*	0.10 *(0.001)*	3.78 *(0.02)*	6.08 *(0.03)*	−0.15 *(0.01)*	2.87 *(0.05)*	5.17 *(0.06)*
	2015	−0.12 *(0.02)*	−0.44 *(0.06)*	0.09 *(0.001)*	3.38 *(0.02)*	5.42 *(0.03)*	−0.03 *(0.02)*	2.93 *(0.06)*	4.98 *(0.06)*
ST_{sum}	2014	28 *(1)*	103 *(2)*	0.9 *(0.02)*	34 *(1)*	54 *(1)*	29 *(1)*	137 *(2)*	157 *(2)*
	2015	36 *(2)*	132 *(7)*	1.3 *(0.04)*	49 *(1)*	78 *(2)*	37 *(2)*	181 *(7)*	210 *(7)*
ST_{mean}	2014	0.74 *(0.03)*	2.71 *(0.05)*	0.02 *(0.001)*	0.89 *(0.03)*	1.42 *(0.03)*	0.76 *(0.03)*	3.61 *(0.06)*	4.13 *(0.06)*
	2015	0.61 *(0.03)*	2.24 *(0.12)*	0.02 *(0.001)*	0.83 *(0.02)*	1.32 *(0.03)*	0.63 *(0.03)*	3.07 *(0.12)*	3.56 *(0.12)*
GS_{sum}	2014	−167 *(5)*	−613 *(17)*	28 *(0.1)*	1,045 *(4)*	1,680 *(7)*	−139 *(5)*	432 *(17)*	1,067 *(18)*
	2015	−154 *(5)*	−564 *(19)*	24 *(0.1)*	896 *(4)*	1,440 *(7)*	−130 *(5)*	332 *(19)*	876 *(20)*
GS_{mean}	2014	−0.97 *(0.03)*	−3.56 *(0.10)*	0.16 *(0.001)*	6.08 *(0.02)*	9.77 *(0.04)*	−0.81 *(0.03)*	2.51 *(0.10)*	6.20 *(0.11)*
	2015	−1.03 *(0.03)*	−3.79 *(0.13)*	0.16 *(0.001)*	6.01 *(0.03)*	9.66 *(0.05)*	−0.87 *(0.03)*	2.23 *(0.13)*	5.88 *(0.14)*
SF_{sum}	2014	36 *(2)*	132 *(6)*	5.3 *(0.1)*	198 *(3)*	318 *(5)*	41 *(2)*	330 *(7)*	450 *(8)*
	2015	51 *(2)*	187 *(6)*	4.9 *(0.1)*	183 *(3)*	294 *(5)*	56 *(2)*	370 *(7)*	481 *(8)*
SF_{mean}	2014	0.58 *(0.03)*	2.13 *(0.10)*	0.09 *(0.002)*	3.19 *(0.05)*	5.13 *(0.08)*	0.67 *(0.03)*	5.32 *(0.11)*	7.26 *(0.13)*
	2015	0.73 *(0.03)*	2.67 *(0.09)*	0.07 *(0.001)*	2.61 *(0.04)*	4.20 *(0.07)*	0.80 *(0.03)*	5.29 *(0.10)*	6.87 *(0.11)*
W_{sum}	2014	12 *(1)*	44 *(5)*	2.8 *(0.1)*	104 *(3)*	168 *(4)*	15 *(1)*	148 *(6)*	212 *(6)*
	2015	23 *(1)*	84 *(5)*	2.8 *(0.1)*	104 *(2)*	168 *(4)*	26 *(1)*	188 *(5)*	252 *(6)*
W_{mean}	2014	0.13 *(0.01)*	0.47 *(0.05)*	0.03 *(0.001)*	1.12 *(0.03)*	1.81 *(0.04)*	0.16 *(0.01)*	1.59 *(0.06)*	*2.28 (0.07)*
	2015	0.26 *(0.01)*	0.97 *(0.06)*	0.03 *(0.001)*	1.20 *(0.02)*	1.93 *(0.05)*	0.30 *(0.01)*	2.16 *(0.06)*	*2.90 (0.07)*

Note. A, annual; ST, soil thawing; GS, growing season; SF, soil freezing; W, winter. Numbers in parentheses represent flux uncertainties due to random measurement errors and gap-filling methods.

were positive for 31 out of the 32 months, illustrating that the peatland was mostly a net source of net CO_2-eq over the monthly scale (Figure S4).

3.3. Seasonal, Annual, and Between-Year Variability of CO_2-eq Fluxes

The net CO_2-eq flux (GWP-28) during the SF period accounted for 33% of the annual net CO_2-eq value (GWP-28), comparable to the contribution from the growing season (Table 1). Moreover, the net CO_2-eq (GWP-28) emission during the wintertime was 14% and 18% of the annual CO_2-eq sums during 2014 and 2015, respectively. In both years, the net CO_2-eq flux contribution from the short ST periods (Table S1) was similar to the long winter seasons, thus showing a twice higher daily net CO_2-eq emission rate on average (Table 1). In contrast, the SGWP-45 metric showed the most significant net CO_2-eq emissions occurring during the growing seasons, 57% and 48% during 2014 and 2015, respectively (Table 1).

For each annual period, Hongyuan peatland acted as a sink for atmospheric CO_2 but a source of CH_4 to the atmosphere (Table 1). While considering the GWP-28 of CH_4, the annual CO_2-eq flux will be 1,047 and 1,071 g CO_2-eq m^{-2} yr^{-1} during 2014 and 2015, respectively, which was almost doubled when applying the SGWP-45 metric (Table 1). The slightly increased annual net CO_2-eq emission during 2015 corresponded with the reduced CO_2 uptake and slightly lower CH_4 emission, compared to the year of 2014. Moreover, the small between-year annual CO_2-eq flux difference (24 g CO_2-eq m^{-2} yr^{-1}) originated from the comparable between-year variabilities during the growing season (−100 g CO_2-eq m^{-2}) and the non-growing seasons (124 g CO_2-eq m^{-2}).

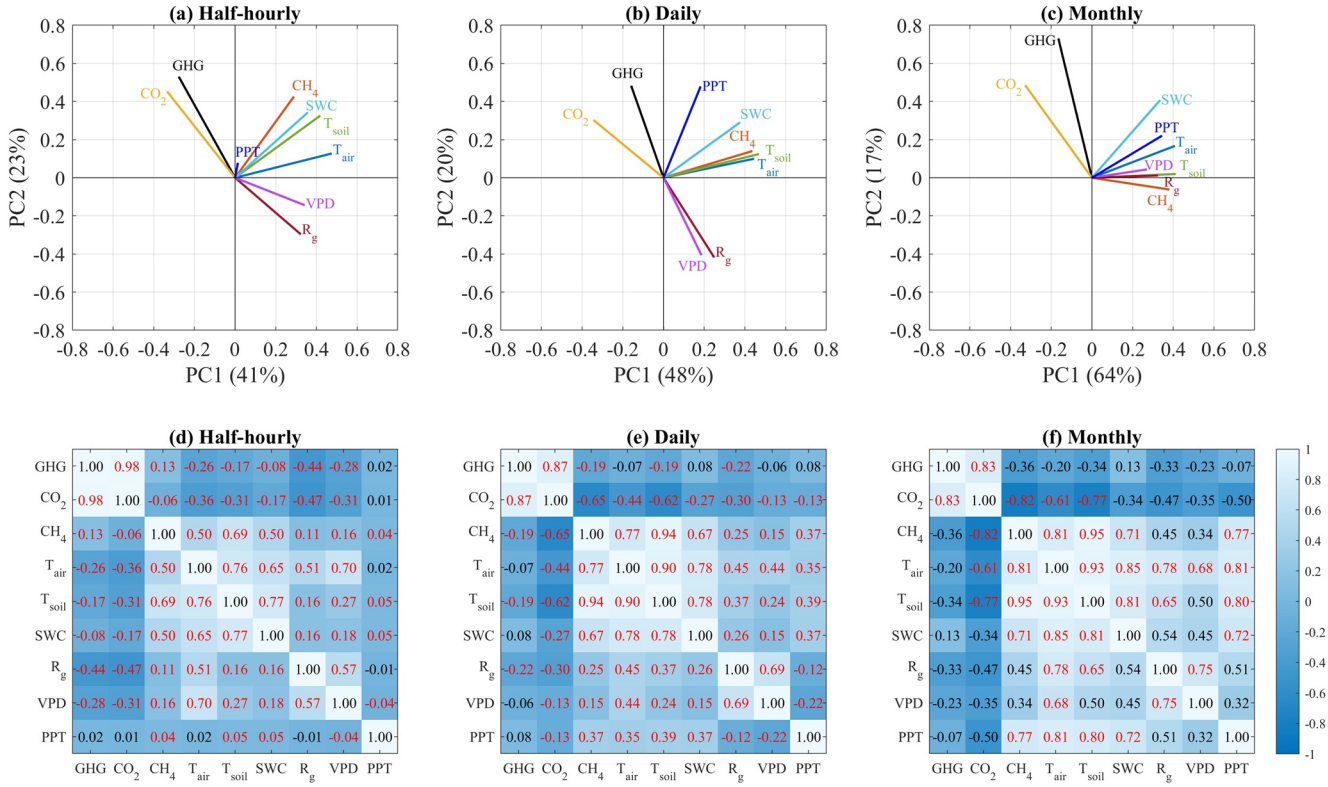

Figure 4. PCA loading plots (a–c) of the correlation structures of GHG (net CO_2-eq, GWP-28), CO_2, and CH_4 (CO_2-eq, GWP-28) fluxes, and measured environmental variables and their correlation matrix (d–e) at half-hourly, daily, and monthly temporal scales. Environmental variables include global radiation (R_g), air temperature (T_{air}), precipitation (PPT), vapor pressure deficit (VPD), and soil temperature (T_{soil}) and soil water content (SWC) both at the depth of 10 cm measured during the study period from December 2013 to July 2016 at Hongyuan peatland. Values in the correlation matrix are the correlation coefficients and significant correlations ($p < 0.001$) are labeled using the red fonts.

3.4. Controlling Factors of Net CO_2-eq Flux

During the study period, the net CO_2-eq flux dominantly varied with the CO_2 flux component at half-hourly ($r = 0.98$, $p < 0.001$), daily ($r = 0.87$, $p < 0.001$), and monthly ($r = 0.83$, $p < 0.001$) timescales, whereas little correlation existed between net CO_2-eq and CH_4 flux at all three temporal scales (Figure 4). The positive correlation between CO_2 uptake and CH_4 emissions increased from half-hourly to monthly scales (Figures 4d–4f). At the half-hourly scale, the cross-correlation showed that the highest correlation ($r = -0.33$) between CO_2 and CH_4 fluxes was achieved when a time lag of 4.5 h (CH_4 flux in +4.5 h) was considered.

Among the six investigated environmental variables, R_g was the strongest controlling factor of the half-hourly CO_2 flux and T_{soil} was the most influencing parameter of the half-hourly CH_4 flux (Figures 4a and 4d). At the coarser temporal resolutions, that is, daily and monthly timescales, T_{soil} became the most influencing abiotic control of both CO_2 and CH_4 fluxes (Figure 4b, 4c, 4e and 4f). Overall, R_g was the dominant environmental factor influencing net CO_2-eq fluxes (GWP-28) at half-hourly and daily intervals (Figures 4d and 4e); however, no significant environmental control was found for the monthly net CO_2-eq flux (Figure 4f). Following the SWGP-45 metric, the correlation structures did not vary much from the GWP-28 metric, except that SWC was significantly correlated with the daily and monthly net CO_2-eq fluxes (Figure S5).

During the growing season, bin-averaged responses of net CO_2-eq fluxes to different R_g classes illustrated that the net CO_2-eq uptake (negative CO_2-eq flux) was significantly enhanced by the increasing R_g before reaching light saturation where R_g was around 500 W m^{-2} (Figure 5a). Meanwhile, T_{air} (5–15°C) and intermediate PPT (15–25 mm d^{-1}) positively affected the net CO_2-eq uptake and emission rates, respectively (Figures 5b and 5c). The relationship between net CO_2-eq flux and VPD showed that the net CO_2-eq uptake quickly increased with VPD up to a threshold of ~0.66 kPa, beyond which the net CO_2-eq uptake started to decrease (Figure 5d). Additionally, the net CO_2-eq flux during the growing season showed similar responses

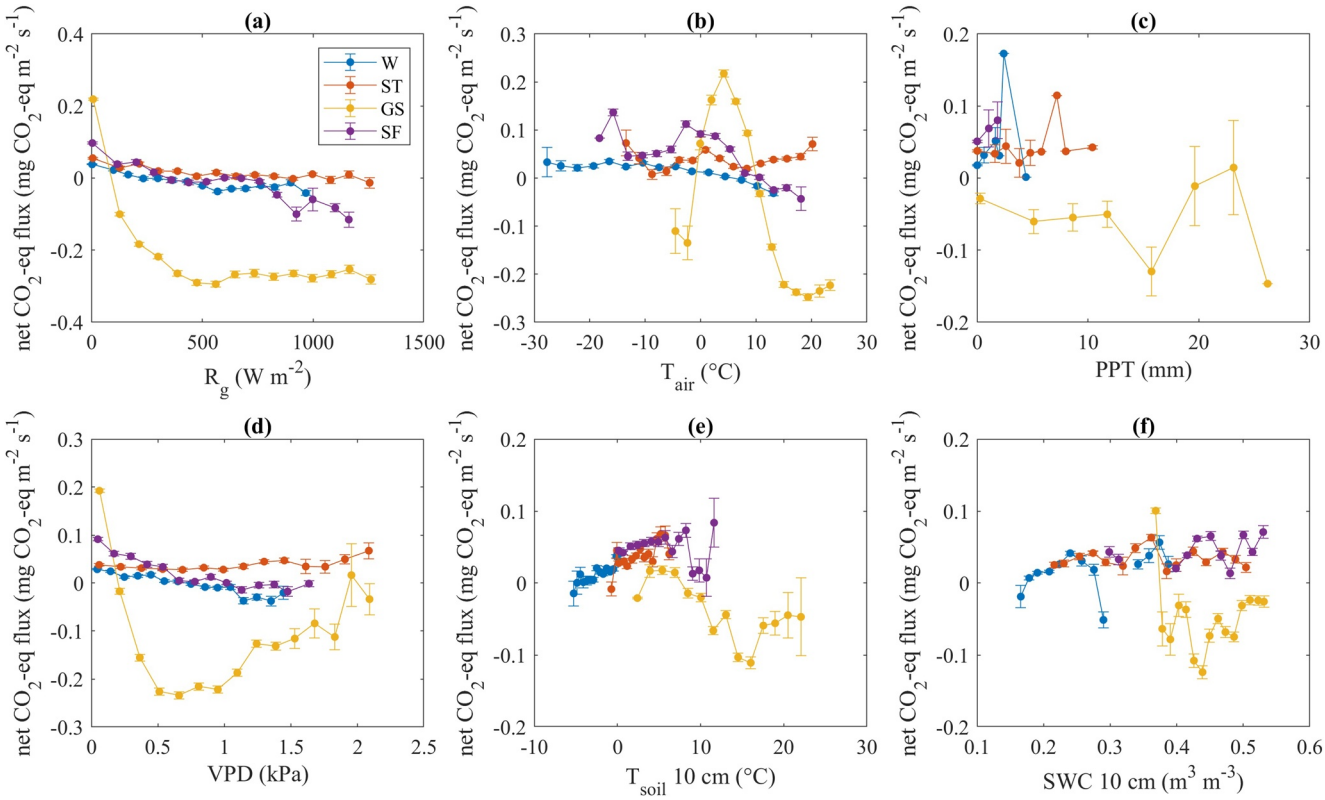

Figure 5. Bin-averaged half-hourly (or daily for PPT) net CO_2-eq flux (GWP-28) against environmental variables during the periods of winter (W), soil thawing (ST), growing season (GS), and soil freezing (SF) at Hongyuan peatland. The error bars show the standard errors of the bin averages.

to T_{soil} (>5°C) and SWC (>0.44 m^3 m^{-3}) as to T_{air} and PPT, respectively (Figures 5e and 5f). During the non-growing seasons, net CO_2-eq generally increased with the rising T_{soil} and with the increasing SWC at the lower range (e.g., 0.16–0.26) (Figures 5e and 5f).

As the CO_2 flux component was dominantly driving the variations in net CO_2-eq fluxes, its sensitivity to the environmental parameters was similar to the responses of net CO_2-eq flux (Figure S6). Whereas for CH_4 flux, we observed that CH_4 emissions during the growing season were linearly increasing with T_{soil} and exponentially increasing with T_{air}, which were also inhibited at the high VPD range (>1.7 kPa; Figure S7). Moreover, CH_4 emission sensitivities to R_g, T_{soil}, and SWC were noted only during the SF period. The environmental responses of net CO_2-eq fluxes for the SGWP-45 metric did not differ much from the GWP-28 metric (Figure S8).

4. Discussion

4.1. CH_4 Emissions Offset the Net Cooling Effect of CO_2 Uptake

On an annual basis, our CO_2 and CH_4 flux measurements demonstrated that Hongyuan peatland was a net sink for atmospheric CO_2, a source of atmospheric CH_4, and an overall net C sink. The mean annual net C sink strength (33 g C m^{-2} yr^{-1}) during the study period was close to the range of C accumulation rates (35–171 g C m^{-2} yr^{-1}) during the recent decades for the alpine peatlands in the Ruoergai Basin (e.g., Hao et al., 2011; X. Liu et al., 2019; Wang et al., 2015), which further confirms that the recent C accumulation rates of peatlands in this region are higher than their Holocene averaged values (Wang et al., 2015; Y. Zhao et al., 2014). Within the C balance, C loss via CH_4 emissions was relatively lower compared to the magnitude of net CO_2 uptake.

While considering the GWP and SGWP of CH_4 over the 100-year timescale, CH_4 emissions have exceeded the net cooling effect of CO_2 uptake by 4.1 and 7.7 times (GWP-28) and 6.6 and 12 times (SGWP-45) for

2014 and 2015, respectively, resulting in the net positive radiative forcing and a potential warming effect of Hongyuan peatland. Considering the warming potential of CH_4 over the 20-year time horizon (GWP and SGWP were 84 and 96, respectively) is ~4 times stronger than that over a 100-year timescale, the GHG emissions from Hongyuan peatland would have a more substantial warming effect over a shorter timescale (e.g., decades). It is thus expected that the alpine peatlands are accelerators of global warming despite they are net C sinks in the meantime. Future studies assessing the peatland radiative forcing should account for the land-atmosphere exchanges of both CO_2 and CH_4.

A large portion (~49% and 38% for GWP-28 and SGWP-45) of the annual net CO_2-eq flux was observed during the SF and winter periods when the environmental conditions were unfavorable for plant growth. During these cold periods, soil respiration was expected to be the dominant process that released CO_2 into the atmosphere (X. Liu et al., 2019), and meanwhile, the peatland was still emitting CH_4 via anaerobic decomposition of soil organic matters (Peng et al., 2019). Moreover, winter was not dormant in terms of CO_2 and CH_4 production, even though T_{soil} at 10 cm depth and T_{air} dropped below zero for 98% and 76% of the wintertime of 2014 and 2015, respectively. During the wintertime, CO_2 and CH_4 emissions from peatlands can still occur through the frozen or snow-covered soils via diffusion and transportation through the chimney effect led by dead plant tissues and ice cracks and also through the burst emissions caused by rapid ST and freezing (Alm et al., 1999; Mastepanov et al., 2008; C. Song et al., 2020). The large amounts of CO_2-eq emissions during the non-growing season were in accordance with previous studies, which have recently highlighted that the overall C and GHG budgets may be underestimated without an accurate assessment for the non-growing season emissions (Aurela et al., 2002; Commane et al., 2017; Natali et al., 2019; W. Song et al., 2015).

4.2. Abiotic Controls of Net CO_2-eq Flux

Compared to 2014, the comparable annual CO_2-eq source strength during 2015 was attributed to the elevated CO_2-eq emissions during the non-growing seasons and slightly reduced net CO_2 uptake during the growing season. Our PCA and sensitivity analyses revealed that global radiation and soil temperature were the primary influencing factors of net CO_2-eq flux variabilities. More specifically, we found that clouds (indicated by low R_g) strongly reduced the net CO_2-eq uptake by blocking the incoming solar radiation and thus primarily reducing photosynthesis (Alton, 2008; Nijp et al., 2015). Meanwhile, precipitation could also stimulate soil respiration during the drier years (e.g., 2015 in this study) due to the increased soil moisture (e.g., Bubier et al., 2003; Juszczak et al., 2013) and thus contributed to the overall reduced net CO_2 uptake (Figure S6f). Additionally, the higher SWC associated with a higher water table level during the ST and winter periods in 2015 could maintain anaerobic conditions and thus have primarily stimulated CH_4 emissions from the peatland compared to the other two years (Figures S7, S9, and S10).

Low soil temperature was expected to slow down the processes of photosynthesis, ecosystem respiration, and CH_4 production simultaneously in peatland ecosystems (Figures S6 and S7). However, the positive correlation between T_{soil} and net CO_2-eq uptake during the growing season indicated its primary role in enhancing photosynthesis relative to CO_2 and CH_4 emissions at the alpine peatlands in the QTP region (Hao et al., 2011). This also explained the between-year variability of net CO_2-eq uptake (Figures S9–S12). Indeed, the observed positive effect of T_{soil} on CH_4 emissions (Figure S7), which has been widely found in this region (e.g., Chen et al., 2008; W. Song et al., 2015) and worldwide (e.g., Dalmagro et al., 2019; Drollinger et al., 2019; Treat et al., 2014; J. Zhao et al., 2016), amplified the sensitivity of net CO_2-eq emission to T_{soil} during the non-growing season but did not switch the overall relationship between net CO_2-eq and T_{soil} during the growing season.

Furthermore, the net CO_2-eq uptake was inhibited under hot and dry conditions (i.e., high VPD) as a result of the declined CH_4 emissions and net CO_2 uptake (Figures S6 and S7). As CO_2 and CH_4 fluxes were tightly coupled at daily and monthly scales due to their strong connection in biogeochemical processes (Figure S13), we also found that higher CO_2 uptake could lead to higher CH_4 production in peatland ecosystems, most likely due to the promoted root exudates (Hatala et al., 2012; Shoemaker et al., 2012). Therefore, it is critical to investigate the environmental controls on the net CO_2-eq flux that integrated the soil biogeochemical and plant physiological processes.

4.3. C and GHG Budgets of Alpine Peatlands on the QTP Under Global Change

The alpine peatlands on the QTP typically act as net C sinks considering the C gains and losses involved in the biogeochemical and physiological processes in the peatland ecosystem (Chen et al., 2014; X. Liu et al., 2019). However, peatlands can be strong sources of net CO_2-eq and thus result in net positive radiative forcing while taking the GWP and SGWP of other GHGs into account. As peatlands in this region could also be significant sources of N_2O (e.g., Chen et al., 2013; H. Liu et al., 2019; Marushchak et al., 2011), which has 265 times stronger GWP than CO_2, the net positive radiative forcing of alpine peatlands on QTP would be further enhanced if combining N_2O flux into the GHG budget. Besides, as the CO_2 and CH_4 exported through stream discharge could account for ~10% of the land-atmosphere C fluxes (Nilsson et al., 2008), the positive radiative forcing of Ruoergai peatlands would be stronger if these exports are included in the C and radiative balances. One recent model study also showed similar results to this study that the significant CH_4 emissions from wetlands even offset the entire regional GHG balance on the QTP (Jin et al., 2015). Therefore, the non-CO_2 GHG emissions from peatlands play an important role in the regional GHG budgets by potentially switching the alpine peatlands from a radiative cooling to a warming effect.

The C and GHG balances of the Ruoergai peatland are sensitive to the rapid climate warming on the QTP, which has been widely observed during the last decades (Yang et al., 2014; T. Yao et al., 2012; You et al., 2016). As the warmer temperature has been found to accelerate CH_4 emissions from peatlands in the Ruoergai Basin by promoting both anaerobic and aerobic metabolisms (Cui et al., 2015; Yang et al., 2014), it is expected that the Ruoergai peatland will emit more CH_4 to the atmosphere and result in more offsetting to both the radiative cooling effect and the carbon sink strength of peatland ecosystems in a projected future warming scenario of the QTP region (L. Zhao et al., 2010) if other influencing factors (e.g., management practices, water balance, etc.) remain similar. In addition, glacier melting and permafrost thawing in response to the rising temperature could lead to more peatland formations in this region (Luan et al., 2018; T. Yao et al., 2012), which will create more CH_4 emission hotspots in the future.

Due to the intensified human disturbance in the QTP region, many peatlands have been drained for animal husbandry or mined for fuels (Chen et al., 2014; L. Yao et al., 2011). Rapid increases in runoff have caused many river diversions and thus incised extensive amounts of peatlands, leading to enhanced regional peatland drainage (Li et al., 2015). Drainage can further alter the GHG and C balances by affecting hydrology, soil, and vegetation composition in the degraded peatland ecosystems (Gyimah et al., 2020). It has been observed that the increased soil temperature and decreased SWC altered by peatland drainage could reduce CH_4 emissions and net CO_2 uptake in the QTP region (Yang et al., 2014, 2017; Zhou et al., 2017), which would further strengthen the positive radiative forcing of these alpine peatlands. Therefore, investigations on the effects of peatland drainage and restoration are greatly needed to identify the role of alpine peatlands in regional and global C and GHG cycles under the circumstances of climate change and anthropogenic disturbances in the future.

5. Conclusions

During the study period, our 32-month EC flux measurements showed that the typical alpine peatland on the eastern QTP acted as a net sink for atmospheric CO_2, a net CH_4 source, and an overall net C sink. When considering their potential influence on radiative forcing, the CH_4 emissions considerably offset the radiative cooling effect of the peatland net CO_2 uptake, thus switching the peatland to a net CO_2-eq source and causing a potentially warming effect. Our analysis further demonstrates that global radiation and soil temperature were the main environmental drivers that influenced the alpine peatland net CO_2-eq flux variabilities from half-hourly to annual timescales. Besides, we found that both CH_4 and CO_2 emissions during the SF and winter periods have contributed significantly to the annual net CO_2-eq fluxes, suggesting that the non-growing season C emissions are extremely important for assessing the overall C and GHG budgets of the alpine peatlands in the QTP region, particularly in a warming climate. The extended long-term continuous GHG monitoring is advocated to further investigate the feedback between the alpine peatlands and global change.

Data Availability Statement

Data sets and codes for this study are available at the archival repository: https://doi.org/10.6084/m9.figshare.15164310.v1, https://doi.org/10.6084/m9.figshare.14619186.v2, https://doi.org/10.6084/m9.figshare.14619228.v2, and https://doi.org/10.6084/m9.figshare.14619237.v2.

Acknowledgments
This study was funded by the Strategic Priority Research Program of the Chinese Academy of Sciences (Grant no. XDB40010300), the National Natural Science Foundation of China (Grant nos. 41907288, 41673119, and 41773140), and the Science and Technology Foundation of Guizhou Province (Grant nos. [2019]1317 and [2020]1Y193). Haijun Peng was supported by the "Light of West China" Program and the CAS Scholarship. J. C. gratefully acknowledges funding from the Kempe Foundations (Grant no. SMK-1743).

References

Alm, J., Saarnio, S., Nykänen, H., Silvola, J., & Martikainen, P. J. (1999). Winter CO_2, CH_4 and N_2O fluxes on some natural and drained boreal peatlands. *Biogeochemistry*, *44*(2), 163–186. https://doi.org/10.1023/A:1006074606204

Alton, P. B. (2008). Reduced carbon sequestration in terrestrial ecosystems under overcast skies compared to clear skies. *Agricultural and Forest Meteorology*, *148*(10), 1641–1653. https://doi.org/10.1016/j.agrformet.2008.05.014

Aurela, M., Laurila, T., & Tuovinen, J.-P. (2002). Annual CO_2 balance of a subarctic fen in northern Europe: Importance of the wintertime efflux. *Journal of Geophysical Research - D: Atmospheres*, *107*(D21), ACH 17-1–ACH 17-12. https://doi.org/10.1029/2002jd002055

Baldocchi, D., & Penuelas, J. (2019). The physics and ecology of mining carbon dioxide from the atmosphere by ecosystems. *Global Change Biology*, *25*(4), 1191–1197. https://doi.org/10.1111/gcb.14559

Bridgham, S. D., Cadillo-Quiroz, H., Keller, J. K., & Zhuang, Q. (2013). Methane emissions from wetlands: Biogeochemical, microbial, and modeling perspectives from local to global scales. *Global Change Biology*, *19*(5), 1325–1346. https://doi.org/10.1111/gcb.12131

Bubier, J., Crill, P., Mosedale, A., Frolking, S., & Linder, E. (2003). Peatland responses to varying interannual moisture conditions as measured by automatic CO_2 chambers. *Global Biogeochemical Cycles*, *17*(2). https://doi.org/10.1029/2002GB001946

Burba, G. G., McDermitt, D. K., Grelle, A., Anderson, D. J., & Xu, L. (2008). Addressing the influence of instrument surface heat exchange on the measurements of CO_2 flux from open-path gas analyzers. *Global Change Biology*, *14*(8), 1854–1876. https://doi.org/10.1111/j.1365-2486.2008.01606.x

Carlson, K. M., Curran, L. M., Asner, G. P., Pittman, A. M., Trigg, S. N., & Marion Adeney, J. (2013). Carbon emissions from forest conversion by Kalimantan oil palm plantations. *Nature Climate Change*, *3*(3), 283–287. https://doi.org/10.1038/nclimate1702

Chaudhary, N., Miller, P. A., & Smith, B. (2017). Modelling past, present and future peatland carbon accumulation across the pan-Arctic region. *Biogeosciences*, *14*(18), 4023–4044. https://doi.org/10.5194/bg-14-4023-2017

Chen, H., Liu, X., Xue, D., Zhu, D., Zhan, W., Li, W., et al. (2021). Methane emissions during different freezing-thawing periods from a fen on the Qinghai-Tibetan Plateau: Four years of measurements. *Agricultural and Forest Meteorology*, *297*, 108279. https://doi.org/10.1016/j.agrformet.2020.108279

Chen, H., Yang, G., Peng, C., Zhang, Y., Zhu, D., Zhu, Q., et al. (2014). The carbon stock of alpine peatlands on the Qinghai-Tibetan Plateau during the Holocene and their future fate. *Quaternary Science Reviews*, *95*, 151–158. https://doi.org/10.1016/j.quascirev.2014.05.003

Chen, H., Yao, S., Wu, N., Wang, Y., Luo, P., Tian, J., et al. (2008). Determinants influencing seasonal variations of methane emissions from alpine wetlands in Zoige Plateau and their implications. *Journal of Geophysical Research - D: Atmospheres*, *113*(D12). https://doi.org/10.1029/2006jd008072

Chen, H., Zhu, Q., Peng, C., Wu, N., Wang, Y., Fang, X., et al. (2013). The impacts of climate change and human activities on biogeochemical cycles on the Qinghai-Tibetan Plateau. *Global Change Biology*, *19*(10), 2940–2955. https://doi.org/10.1111/gcb.12277

Commane, R., Lindaas, J., Benmergui, J., Luus, K. A., Chang, R. Y.-W., Daube, B. C., et al. (2017). Carbon dioxide sources from Alaska driven by increasing early winter respiration from Arctic tundra. *Proceedings of the National Academy of Sciences of the United States of America*, *114*(21), 5361–5366. https://doi.org/10.1073/pnas.1618567114

Cui, M., Ma, A., Qi, H., Zhuang, X., Zhuang, G., & Zhao, G. (2015). Warmer temperature accelerates methane emissions from the Zoige wetland on the Tibetan Plateau without changing methanogenic community composition. *Scientific Reports*, *5*(1), 11616. https://doi.org/10.1038/srep11616

Dalmagro, H. J., Zanella de Arruda, P. H., Vourlitis, G. L., Lathuillière, M. J., Nogueira, J. d. S., Couto, E. G., & Johnson, M. S. (2019). Radiative forcing of methane fluxes offsets net carbon dioxide uptake for a tropical flooded forest. *Global Change Biology*, *25*(6), 1967–1981. https://doi.org/10.1111/gcb.14615

Dommain, R., Frolking, S., Jeltsch-Thömmes, A., Joos, F., Couwenberg, J., & Glaser, P. H. (2018). A radiative forcing analysis of tropical peatlands before and after their conversion to agricultural plantations. *Global Change Biology*, *24*(11), 5518–5533. https://doi.org/10.1111/gcb.14400

Drollinger, S., Maier, A., & Glatzel, S. (2019). Interannual and seasonal variability in carbon dioxide and methane fluxes of a pine peat bog in the Eastern Alps, Austria. *Agricultural and Forest Meteorology*, *275*, 69–78. https://doi.org/10.1016/j.agrformet.2019.05.015

Fan, S. M., Wofsy, S. C., Bakwin, P. S., Jacob, D. J., & Fitzjarrald, D. R. (1990). Atmosphere-biosphere exchange of CO_2 and O_3 in the central Amazon forest. *Journal of Geophysical Research*, *95*(D10), 16851–16864. https://doi.org/10.1029/JD095iD10p16851

Fenner, N., & Freeman, C. (2011). Drought-induced carbon loss in peatlands. *Nature Geoscience*, *4*(12), 895–900. https://doi.org/10.1038/ngeo1323

Finkelstein, P. L., & Sims, P. F. (2001). Sampling error in eddy correlation flux measurements. *Journal of Geophysical Research*, *106*(D4), 3503–3509. https://doi.org/10.1029/2000JD900731

Friedlingstein, P., Jones, M. W., O'Sullivan, M., Andrew, R. M., Hauck, J., Peters, G. P., et al. (2019). Global carbon budget 2019. *Earth System Science Data*, *11*(4), 1783–1838. https://doi.org/10.5194/essd-11-1783-2019

Frolking, S., & Roulet, N. T. (2007). Holocene radiative forcing impact of northern peatland carbon accumulation and methane emissions. *Global Change Biology*, *13*(5), 1079–1088. https://doi.org/10.1111/j.1365-2486.2007.01339.x

Frolking, S., Talbot, J., Jones, M. C., Treat, C. C., Kauffman, J. B., Tuittila, E.-S., & Roulet, N. (2011). Peatlands in the Earth's 21st century climate system. *Environmental Reviews*, *19*, 371–396. https://doi.org/10.1139/a11-014

Gash, J. H. C., & Culf, A. D. (1996). Applying a linear detrend to eddy correlation data in realtime. *Boundary-Layer Meteorology*, *79*(3), 301–306. https://doi.org/10.1007/bf00119443

Gyimah, A., Wu, J., Scott, R., & Gong, Y. (2020). Agricultural drainage increases the photosynthetic capacity of boreal peatlands. *Agriculture, Ecosystems & Environment*, *300*, 106984. https://doi.org/10.1016/j.agee.2020.106984

Hao, Y. B., Cui, X. Y., Wang, Y. F., Mei, X. R., Kang, X. M., Wu, N., et al. (2011). Predominance of precipitation and temperature controls on ecosystem CO_2 exchange in Zoige Alpine Wetlands of southwest China. *Wetlands*, *31*(2), 413–422. https://doi.org/10.1007/s13157-011-0151-1

Hatala, J. A., Detto, M., & Baldocchi, D. D. (2012). Gross ecosystem photosynthesis causes a diurnal pattern in methane emission from rice. *Geophysical Research Letters*, *39*(6). https://doi.org/10.1029/2012gl051303

Hemes, K. S., Chamberlain, S. D., Eichelmann, E., Anthony, T., Valach, A., Kasak, K., et al. (2019). Assessing the carbon and climate benefit of restoring degraded agricultural peat soils to managed wetlands. *Agricultural and Forest Meteorology*, *268*, 202–214. https://doi.org/10.1016/j.agrformet.2019.01.017

Hemes, K. S., Chamberlain, S. D., Eichelmann, E., Knox, S. H., & Baldocchi, D. D. (2018). A biogeochemical compromise: The high methane cost of sequestering carbon in restored wetlands. *Geophysical Research Letters*, *45*(12), 6081–6091. https://doi.org/10.1029/2018GL077747

Hong, Y. T., Hong, B., Lin, Q. H., Shibata, Y., Hirota, M., Zhu, Y. X., et al. (2005). Inverse phase oscillations between the East Asian and Indian Ocean summer monsoons during the last 12000 years and paleo-El Niño. *Earth and Planetary Science Letters*, *231*(3), 337–346. https://doi.org/10.1016/j.epsl.2004.12.025

Hopple, A. M., Wilson, R. M., Kolton, M., Zalman, C. A., Chanton, J. P., Kostka, J., et al. (2020). Massive peatland carbon banks vulnerable to rising temperatures. *Nature Communications*, *11*(1), 2373. https://doi.org/10.1038/s41467-020-16311-8

Jin, Z., Zhuang, Q., He, J.-S., Zhu, X., & Song, W. (2015). Net exchanges of methane and carbon dioxide on the Qinghai-Tibetan Plateau from 1979 to 2100. *Environmental Research Letters*, *10*(8), 085007. https://doi.org/10.1088/1748-9326/10/8/085007

Johansson, T., Malmer, N., Crill, P. M., Friborg, T., Åkerman, J. H., Mastepanov, M., & Christensen, T. R. (2006). Decadal vegetation changes in a northern peatland, greenhouse gas fluxes and net radiative forcing. *Global Change Biology*, *12*(12), 2352–2369. https://doi.org/10.1111/j.1365-2486.2006.01267.x

Juszczak, R., Humphreys, E., Acosta, M., Michalak-Galczewska, M., Kayzer, D., & Olejnik, J. (2013). Ecosystem respiration in a heterogeneous temperate peatland and its sensitivity to peat temperature and water table depth. *Plant and Soil*, *366*(1), 505–520. https://doi.org/10.1007/s11104-012-1441-y

Kirschke, S., Bousquet, P., Ciais, P., Saunois, M., Canadell, J. G., Dlugokencky, E. J., et al. (2013). Three decades of global methane sources and sinks. *Nature Geoscience*, *6*(10), 813–823. https://doi.org/10.1038/ngeo1955

Kljun, N., Calanca, P., Rotach, M. W., & Schmid, H. P. (2015). A simple two-dimensional parameterisation for Flux Footprint Prediction (FFP). *Geoscientific Model Development*, *8*(11), 3695–3713. https://doi.org/10.5194/gmd-8-3695-2015

Li, Z.-W., Wang, Z.-Y., Brierley, G., Nicoll, T., Pan, B.-Z., & Li, Y.-F. (2015). Shrinkage of the Ruoergai Swamp and changes to landscape connectivity, Qinghai-Tibet Plateau. *Catena*, *126*, 155–163. https://doi.org/10.1016/j.catena.2014.10.035

Liu, H., Zak, D., Rezanezhad, F., & Lennartz, B. (2019). Soil degradation determines release of nitrous oxide and dissolved organic carbon from peatlands. *Environmental Research Letters*, *14*(9), 094009. https://doi.org/10.1088/1748-9326/ab3947

Liu, J., Zhou, Y., Valach, A., Shortt, R., Kasak, K., Rey-Sanchez, C., et al. (2020). Methane emissions reduce the radiative cooling effect of a subtropical estuarine mangrove wetland by half. *Global Change Biology*, *26*, 4998–5016. https://doi.org/10.1111/gcb.15247

Liu, X., Zhu, D., Zhan, W., Chen, H., Zhu, Q., Hao, Y., et al. (2019). Five-year measurements of net ecosystem CO_2 exchange at a fen in the Zoige peatlands on the Qinghai-Tibetan Plateau. *Journal of Geophysical Research - D: Atmospheres*, *124*(22), 11803–11818. https://doi.org/10.1029/2019jd031429

Loisel, J., van Bellen, S., Pelletier, L., Talbot, J., Hugelius, G., Karran, D., et al. (2017). Insights and issues with estimating northern peatland carbon stocks and fluxes since the Last Glacial Maximum. *Earth-Science Reviews*, *165*, 59–80. https://doi.org/10.1016/j.earscirev.2016.12.001

Luan, J., Liu, S., Wu, J., Wang, M., & Yu, Z. (2018). The transient shift of driving environmental factors of carbon dioxide and methane fluxes in Tibetan peatlands before and after hydrological restoration. *Agricultural and Forest Meteorology*, *250–251*, 138–146. https://doi.org/10.1016/j.agrformet.2017.12.248

Lund, M., Lafleur, P. M., Roulet, N. T., Lindroth, A., Christensen, T. R., Aurela, M., et al. (2010). Variability in exchange of CO_2 across 12 northern peatland and tundra sites. *Global Change Biology*, *16*(9), 2436. https://doi.org/10.1111/j.1365-2486.2009.02104.x

Marushchak, M. E., Pitkämäki, A., Koponen, H., Biasi, C., Seppälä, M., & Martikainen, P. J. (2011). Hot spots for nitrous oxide emissions found in different types of permafrost peatlands. *Global Change Biology*, *17*(8), 2601–2614. https://doi.org/10.1111/j.1365-2486.2011.02442.x

Mastepanov, M., Sigsgaard, C., Dlugokencky, E. J., Houweling, S., Ström, L., Tamstorf, M. P., & Christensen, T. R. (2008). Large tundra methane burst during onset of freezing. *Nature*, *456*(7222), 628–630. https://doi.org/10.1038/nature07464

Mathijssen, P. J. H., Kähkölä, N., Tuovinen, J.-P., Lohila, A., Minkkinen, K., Laurila, T., & Väliranta, M. (2017). Lateral expansion and carbon exchange of a boreal peatland in Finland resulting in 7000 years of positive radiative forcing. *Journal of Geophysical Research: Biogeosciences*, *122*(3), 562–577. https://doi.org/10.1002/2016JG003749

Mauder, M., & Foken, T. (2004). *Documentation and instruction manual of the eddy covariance software package TK2* (pp. 1–67)

Minkkinen, K., Korhonen, R., Savolainen, I., & Laine, J. (2002). Carbon balance and radiative forcing of Finnish peatlands 1900–2100 – The impact of forestry drainage. *Global Change Biology*, *8*(8), 785–799. https://doi.org/10.1046/j.1365-2486.2002.00504.x

Moncrieff, J. B., Clement, R., Finnigan, J., & Meyers, T. (2004). Averaging, detrending, and filtering of Eddy covariance time series. In X. Lee, W. J. Massman, & B. E. Law (Eds.), *Handbook of micrometeorology*. Springer Netherlands

Moncrieff, J. B., Massheder, J. M., de Bruin, H., Elbers, J., Friborg, T., Heusinkveld, B., et al. (1997). A system to measure surface fluxes of momentum, sensible heat, water vapour and carbon dioxide. *Journal of Hydrology*, *188–189*, 589–611. https://doi.org/10.1016/S0022-1694(96)03194-0

Myhre, G., Shindell, D., Bréon, F.-M., Collins, W., Fuglestvedt, J., Huang, J., et al. (2013). Anthropogenic and natural radiative forcing. In T. F. Stocker, D. Qin, G.-K. Plattner, M. Tignor, S. K. Allen, J. Boschung, A. Nauels, Y. Xia, V. Bex, & P. M. Midgley (Eds.), *Climate change 2013: The physical science basis. Contribution of working group I to the fifth assessment report of the intergovernmental panel on climate change*. Cambridge, United Kingdom and New York, NY, USA: Cambridge University Press

Natali, S. M., Watts, J. D., Rogers, B. M., Potter, S., Ludwig, S. M., Selbmann, A.-K., et al. (2019). Large loss of CO_2 in winter observed across the northern permafrost region. *Nature Climate Change*, *9*, 852–857. https://doi.org/10.1038/s41558-019-0592-8

Neubauer, S. C., & Megonigal, J. P. (2015). Moving beyond global warming potentials to quantify the climatic role of ecosystems. *Ecosystems*, *18*(6), 1000–1013. https://doi.org/10.1007/s10021-015-9879-4

Nijp, J. J., Limpens, J., Metselaar, K., Peichl, M., Nilsson, M. B., van der Zee, S. E., & Berendse, F. (2015). Rain events decrease boreal peatland net CO_2 uptake through reduced light availability. *Global Change Biology*, *21*(6), 2309–2320. https://doi.org/10.1111/gcb.12864

Nilsson, M., Sagerfors, J., Buffam, I., Laudon, H., Eriksson, T., Grelle, A., et al. (2008). Contemporary carbon accumulation in a boreal oligotrophic minerogenic mire – A significant sink after accounting for all C-fluxes. *Global Change Biology*, *14*(10), 2317–2332. https://doi.org/10.1111/j.1365-2486.2008.01654.x

Nugent, K. A., Strachan, I. B., Roulet, N. T., Strack, M., Frolking, S., & Helbig, M. (2019). Prompt active restoration of peatlands substantially reduces climate impact. *Environmental Research Letters*, *14*(12), 124030. https://doi.org/10.1088/1748-9326/ab56e6

Papale, D., Reichstein, M., Aubinet, M., Canfora, E., Bernhofer, C., Kutsch, W., et al. (2006). Towards a standardized processing of Net Ecosystem Exchange measured with eddy covariance technique: Algorithms and uncertainty estimation. *Biogeosciences*, *3*(4), 571–583. https://doi.org/10.5194/bg-3-571-2006

Peichl, M., Öquist, M., Löfvenius, M. O., Ilstedt, U., Sagerfors, J., Grelle, A., et al. (2014). A 12-year record reveals pre-growing season temperature and water table level threshold effects on the net carbon dioxide exchange in a boreal fen. *Environmental Research Letters*, *9*(5), 055006. https://doi.org/10.1088/1748-9326/9/5/055006

Peng, H., Guo, Q., Ding, H., Hong, B., Zhu, Y., Hong, Y., et al. (2019). Multi-scale temporal variation in methane emission from an alpine peatland on the Eastern Qinghai-Tibetan Plateau and associated environmental controls. *Agricultural and Forest Meteorology*, *276–277*, 276–277. https://doi.org/10.1016/j.agrformet.2019.107616

Peng, H., Hong, B., Hong, Y., Zhu, Y., Cai, C., Yuan, L., & Wang, Y. (2015). Annual ecosystem respiration variability of alpine peatland on the eastern Qinghai-Tibet Plateau and its controlling factors. *Environmental Monitoring and Assessment*, *187*(9), 550. https://doi.org/10.1007/s10661-015-4733-x

Petrescu, A. M. R., Lohila, A., Tuovinen, J.-P., Baldocchi, D. D., Desai, A. R., Roulet, N. T., et al. (2015). The uncertain climate footprint of wetlands under human pressure. *Proceedings of the National Academy of Sciences of the United States of America*, *112*(15), 4594–4599. https://doi.org/10.1073/pnas.1416267112

Poulter, B., Bousquet, P., Canadell, J. G., Ciais, P., Peregon, A., Saunois, M., et al. (2017). Global wetland contribution to 2000-2012 atmospheric methane growth rate dynamics. *Environmental Research Letters*, *12*(9), 094013. https://doi.org/10.1088/1748-9326/aa8391

Reichstein, M., Falge, E., Baldocchi, D., Papale, D., Aubinet, M., Berbigier, P., et al. (2005). On the separation of net ecosystem exchange into assimilation and ecosystem respiration: Review and improved algorithm. *Global Change Biology*, *11*(9), 1424–1439. https://doi.org/10.1111/j.1365-2486.2005.001002.x

Richardson, A. D., & Hollinger, D. Y. (2007). A method to estimate the additional uncertainty in gap-filled NEE resulting from long gaps in the CO_2 flux record. *Agricultural and Forest Meteorology*, *147*(3–4), 199–208. https://doi.org/10.1016/j.agrformet.2007.06.004

Rinne, J., Tuittila, E.-S., Peltola, O., Li, X., Raivonen, M., Alekseychik, P., et al. (2018). Temporal variation of ecosystem scale methane emission from a boreal fen in relation to temperature, water table position, and carbon dioxide fluxes. *Global Biogeochemical Cycles*, *32*(7), 1087–1106. https://doi.org/10.1029/2017GB005747

Schaefer, H., Fletcher, S. E. M., Veidt, C., Lassey, K. R., Brailsford, G. W., Bromley, T. M., et al. (2016). A 21st-century shift from fossil-fuel to biogenic methane emissions indicated by $^{13}CH_4$. *Science*, *352*(6281), 80–84. https://doi.org/10.1126/science.aad2705

Shoemaker, J. K., Varner, R. K., & Schrag, D. P. (2012). Characterization of subsurface methane production and release over 3 years at a New Hampshire wetland. *Geochimica et Cosmochimica Acta*, *91*, 120–139. https://doi.org/10.1016/j.gca.2012.05.029

Slättberg, N., & Chen, D. (2020). A long-term climatology of planetary boundary layer height over the Tibetan Plateau revealed by ERA5. *Paper presented at EGU General Assembly 2020*.

Song, C., Luan, J., Xu, X., Ma, M., Aurela, M., Lohila, A., et al. (2020). A microbial functional group-based CH_4 model integrated into a terrestrial ecosystem model: Model structure, site-level evaluation, and sensitivity analysis. *Journal of Advances in Modeling Earth Systems*, *12*(4), e2019MS001867. https://doi.org/10.1029/2019ms001867

Song, W., Wang, H., Wang, G., Chen, L., Jin, Z., Zhuang, Q., & He, J.-S. (2015). Methane emissions from an alpine wetland on the Tibetan Plateau: Neglected but vital contribution of the nongrowing season. *Journal of Geophysical Research: Biogeosciences*, *120*(8), 1475–1490. https://doi.org/10.1002/2015jg003043

Stocker, B. D., Yu, Z., Massa, C., & Joos, F. (2017). Holocene peatland and ice-core data constraints on the timing and magnitude of CO_2 emissions from past land use. *Proceedings of the National Academy of Sciences of the United States of America*, *114*(7), 1492–1497. https://doi.org/10.1073/pnas.1613889114

Swindles, G. T., Morris, P. J., Mullan, D. J., Payne, R. J., Roland, T. P., Amesbury, M. J., et al. (2019). Widespread drying of European peatlands in recent centuries. *Nature Geoscience*, *12*(11), 922–928. https://doi.org/10.1038/s41561-019-0462-z

Tang, L., Duan, X., Kong, F., Zhang, F., Zheng, Y., Li, Z., et al. (2018). Influences of climate change on area variation of Qinghai Lake on Qinghai-Tibetan Plateau since 1980s. *Scientific Reports*, *8*(1), 7331. https://doi.org/10.1038/s41598-018-25683-3

Treat, C. C., Wollheim, W. M., Varner, R. K., Grandy, A. S., Talbot, J., & Frolking, S. (2014). Temperature and peat type control CO_2 and CH_4 production in Alaskan permafrost peats. *Global Change Biology*, *20*(8), 2674–2686. https://doi.org/10.1111/gcb.12572

Turetsky, M. R., Benscoter, B., Page, S., Rein, G., van der Werf, G. R., & Watts, A. (2015). Global vulnerability of peatlands to fire and carbon loss. *Nature Geoscience*, *8*(1), 11–14. https://doi.org/10.1038/ngeo2325

Turetsky, M. R., Kotowska, A., Bubier, J., Dise, N. B., Crill, P., Hornibrook, E. R. C., et al. (2014). A synthesis of methane emissions from 71 northern, temperate, and subtropical wetlands, *Global Change Biology*, *20*(7), 2183–2197. https://doi.org/10.1111/gcb.12580

Ueyama, M., Yazaki, T., Hirano, T., Futakuchi, Y., & Okamura, M. (2020). Environmental controls on methane fluxes in a cool temperate bog. *Agricultural and Forest Meteorology*, *281*, 107852. https://doi.org/10.1016/j.agrformet.2019.107852

Wang, M., Yang, G., Gao, Y., Chen, H., Wu, N., Peng, C., et al. (2015). Higher recent peat C accumulation than that during the Holocene on the Zoige Plateau. *Quaternary Science Reviews*, *114*, 116–125. https://doi.org/10.1016/j.quascirev.2015.01.025

Webb, E. K., Pearman, G. I., & Leuning, R. (1980). Correction of flux measurements for density effects due to heat and water-vapor transfer. *Quarterly Journal of the Royal Meteorological Society*, *106*(447), 85–100. https://doi.org/10.1002/qj.49710644707

Wilczak, J. M., Oncley, S. P., & Stage, S. A. (2001). Sonic anemometer tilt correction algorithms. *Boundary-Layer Meteorology*, *99*(1), 127–150. https://doi.org/10.1023/a:1018966204465

WMO. (2018). WMO greenhouse gas bulletin no. 14: The state of greenhouse gases in the atmosphere based on global observations through 2017

Wutzler, T., Lucas-Moffat, A., Migliavacca, M., Knauer, J., Sickel, K., Šigut, L., et al. (2018). Basic and extensible post-processing of eddy covariance flux data with REddyProc. *Biogeosciences*, *15*(16), 5015–5030. https://doi.org/10.5194/bg-15-5015-2018

Xiang, S., Guo, R., Wu, N., & Sun, S. (2009). Current status and future prospects of Zoige Marsh in Eastern Qinghai-Tibet Plateau. *Ecological Engineering*, *35*(4), 553–562. https://doi.org/10.1016/j.ecoleng.2008.02.016

Xu, J., Morris, P. J., Liu, J., & Holden, J. (2018). PEATMAP: Refining estimates of global peatland distribution based on a meta-analysis. *Catena*, *160*, 134–140. https://doi.org/10.1016/j.catena.2017.09.010

Yang, G., Chen, H., Wu, N., Tian, J., Peng, C., Zhu, Q., et al. (2014). Effects of soil warming, rainfall reduction and water table level on CH_4 emissions from the Zoige peatland in China. *Soil Biology and Biochemistry*, *78*, 83–89. https://doi.org/10.1016/j.soilbio.2014.07.013

Yang, G., Peng, C., Chen, H., Dong, F., Wu, N., Yang, Y., et al. (2017). Qinghai-Tibetan Plateau peatland sustainable utilization under anthropogenic disturbances and climate change, Ecosyst. *Health Sustainability*, *3*(3), e01263. https://doi.org/10.1002/ehs2.1263

Yao, L., Zhao, Y., Gao, S., Sun, J., & Li, F. (2011). The peatland area change in past 20 years in the Zoige Basin, eastern Tibetan Plateau. *Frontiers of Earth Science*, *5*(3), 271. https://doi.org/10.1007/s11707-011-0178-x

Yao, T., Thompson, L., Yang, W., Yu, W., Gao, Y., Guo, X., et al. (2012). Different glacier status with atmospheric circulations in Tibetan Plateau and surroundings. *Nature Climate Change*, *2*(9), 663–667. https://doi.org/10.1038/nclimate1580

You, Q., Min, J., & Kang, S. (2016). Rapid warming in the Tibetan Plateau from observations and CMIP5 models in recent decades. *International Journal of Climatology*, *36*(6), 2660–2670. https://doi.org/10.1002/joc.4520

Yu, Z. (2011). Holocene carbon flux histories of the world's peatlands:Global carbon-cycle implications. *The Holocene*, *21*(5), 761–774. https://doi.org/10.1177/0959683610386982

Yu, Z., Loisel, J., Brosseau, D. P., Beilman, D. W., & Hunt, S. J. (2010). Global peatland dynamics since the Last Glacial Maximum. *Geophysical Research Letters*, *37*(13). https://doi.org/10.1029/2010gl043584

Yuan, W., Luo, Y., Liang, S., Yu, G., Niu, S., Stoy, P., et al. (2011). Thermal adaptation of net ecosystem exchange. *Biogeosciences*, *8*(6), 1453–1463. https://doi.org/10.5194/bg-8-1453-2011

Yvon-Durocher, G., Allen, A. P., Bastviken, D., Conrad, R., Gudasz, C., St-Pierre, A., et al. (2014). Methane fluxes show consistent temperature dependence across microbial to ecosystem scales. *Nature*, *507*(7493), 488–491. https://doi.org/10.1038/nature13164

Zhao, J., Peichl, M., & Nilsson, M. B. (2016). Enhanced winter soil frost reduces methane emission during the subsequent growing season in a boreal peatland. *Global Change Biology*, *22*(2), 750–762. https://doi.org/10.1111/gcb.13119

Zhao, L., Li, J., Xu, S., Zhou, H., Li, Y., Gu, S., & Zhao, X. (2010). Seasonal variations in carbon dioxide exchange in an alpine wetland meadow on the Qinghai-Tibetan Plateau. *Biogeosciences*, *7*(4), 1207–1221. https://doi.org/10.5194/bg-7-1207-2010

Zhao, Y., Tang, Y., Yu, Z., Li, H., Yang, B., Zhao, W., et al. (2014). Holocene peatland initiation, lateral expansion, and carbon dynamics in the Zoige Basin of the eastern Tibetan Plateau. *The Holocene*, *24*(9), 1137–1145. https://doi.org/10.1177/0959683614538077

Zhou, W., Cui, L., Wang, Y., & Li, W. (2017). Methane emissions from natural and drained peatlands in the Zoigê, eastern Qinghai-Tibet Plateau. *Journal of Forest Research*, *28*(3), 539–547. https://doi.org/10.1007/s11676-016-0343-x